

# Green Chemistry

Accepted Manuscript



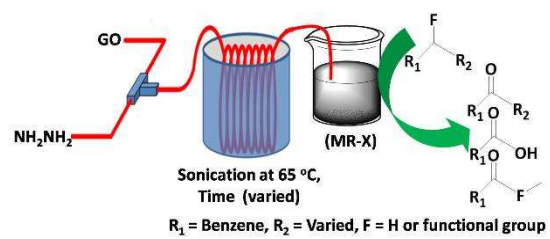
This is an *Accepted Manuscript*, which has been through the Royal Society of Chemistry peer review process and has been accepted for publication.

*Accepted Manuscripts* are published online shortly after acceptance, before technical editing, formatting and proof reading. Using this free service, authors can make their results available to the community, in citable form, before we publish the edited article. We will replace this *Accepted Manuscript* with the edited and formatted *Advance Article* as soon as it is available.

You can find more information about *Accepted Manuscripts* in the [Information for Authors](#).

Please note that technical editing may introduce minor changes to the text and/or graphics, which may alter content. The journal's standard [Terms & Conditions](#) and the [Ethical guidelines](#) still apply. In no event shall the Royal Society of Chemistry be held responsible for any errors or omissions in this *Accepted Manuscript* or any consequences arising from the use of any information it contains.

## Graphical abstract



Cite this: DOI: 10.1039/x0xx00000x

Received 00th January 2014,  
Accepted 00th January 2014

DOI: 10.1039/x0xx00000x

www.rsc.org/

## Eco-efficient preparation of N-doped graphene equivalent and its application to metal free selective oxidation reaction

Ajay K. Singh, K.C Basavaraju, Siddharth Sharma, Seungwook Jang, Chan Pil Park,  
Dong-Pyo Kim\*

Here, we demonstrate that graphene oxide (GO) can be converted to N-doped reduced GO (rGO) that could become a substitute for N-doped graphene. Simultaneous doping and reduction can be accomplished for the purpose by simply mixing GO with hydrazine and then continuously sonicating the solution at 65 °C. A high level of reduction is realized as evidenced by a carbon to oxygen ratio of 20.7 that compares with the highest value of 15.3 ever reported in solution (water + hydrazine) methods. Nitrogen doping is possible up to 6.3 wt% and the extent of doping can be increased with increasing sonication time. Notably, the simple tuning process of N-doping in GO greatly enhanced the efficiency of the carbocatalyst for various kinds of metal free oxidation reactions, and henceforth is proposed as a suitable candidate for future industrial application.

### Introduction

Highly selective catalysts that are readily recycled, cheaper and metal free are vital for the development of sustainable chemical process,<sup>1</sup> moreover, in certain cases, reaction parameters can be carefully tuned to improve process performance. Generally, in case of homogeneous catalysts, the steric and electronic features of novel metals (palladium, rhodium, ruthenium, and iridium) are varied to attain high selectivity.<sup>2</sup> However, the high price and limited availability of these precious metals have spurred interest in metal free catalytic system among the scientific community, especially carbocatalyst, due to more earth-abundant inexpensive alternatives.<sup>3</sup>

By introducing the oxygen, and nitrogen atoms in the carbon network, the steric and electronic features of graphite (semi-metal) could be tuned, which can subsequently be used as equivalent to metal or sometimes as a better alternative to metal catalyst.<sup>4</sup> Engineering of hexagonal crystal-

lattice of graphite sheets through substitutional doping is thereby a direct way to control the steric and electronic properties of graphite. Furthermore, the process remarkably expands its applications in frontiers of catalysis and electronic devices. Bielawski et al. introduced only O heteroatom on graphite layer to make it a suitable candidate for the oxidation reaction.<sup>3</sup> The only drawbacks were low catalytic efficiency, requirement of high loading (60-400 wt%) and low thermal stability during oxidation reaction.<sup>4c</sup> Wang et al. introduced only N atom on graphene layer at high temperature chemical vapour deposition (CVD) process to make carbocatalyst, but the tuning of N and O contents on graphite layer was very limited.<sup>4a</sup> In light of ever-expanding applications of tuned N-doped reduced graphene oxide (rGO) and high throughput availability of GO, it is highly desirable to have a direct and yet efficient approach for simultaneous reduction and N-doping on GO.

Unintentional nitrogen doping was comprehended in an initial attempt to reduce graphite oxide with hydrazine.<sup>5</sup> Hydrazine is highly toxic and dangerously unstable.<sup>6,7</sup> Microfluidic chemical technology is one of the most suitable tools to minimize such toxic and explosive substances owing to their extremely small internal volume and continuous consumption capability.<sup>8</sup> And it can be considered as a greener and sustainable approach towards hydrazine involved chemistry.<sup>9</sup>

To minimize the hydrazine exposure, we present an eco-efficient and simultaneous approach for reduction and nitrogen doping on GO, which yields the highest carbon to oxygen ratio and the highest nitrogen content ever reported in solution methods. We also utilized tuned N-

*National Center of Applied Microfluidic Chemistry  
Department of Chemical Engineering, POSTECH (Pohang University of  
Science and Technology), Pohang, Korea 790-784  
Email: dpkim@postech.ac.kr*

Electronic Supplementary Information (ESI) available: Detailed experimental procedure, catalysts preparation, catalysts characterization, catalytic result, comparative study, catalyst proposed mechanism and the supplementary results. See DOI: 10.1039/c000000x/

doped rGO to expand the horizon of applications to metal-free catalysis for selective oxidation of hydrocarbons, alcohols, bromoalkanes, and oxidative coupling reaction of aminoalkanes to produce the functionalized compounds having exceptional selective ketones, acid, ester, ether and amides using mild oxidants (peroxide) under evergreen water solvent.

## Result and Discussion

To overcome the safety issue and eco-efficient simultaneous reduction and N-doping of GO, we have devised an approach that involves introducing aqueous solutions of GO and hydrazine hydrate into a capillary microreactor and then subjecting the microreactor to sonication (mechanical energy) to induce microsonochemical reduction (MR) process. In addition, as shown in Fig. 1, both T-mixer and Teflon (PTFA) capillary microreactor were placed in the ultrasonic bath (power = 330 W, frequency = 40 KHz, temperature = 65 °C) to circumvent tube-blocking problem, which was encountered initially. The reduced graphene oxide samples in the form of black precipitate were collected at controlled retention times in a range between 30 and 70 min by varying the capillary length with a constant flow rate of 30  $\mu\text{L}/\text{min}$  (see electronic supplementary information (ESI) Table S1). The doped rGO samples thus obtained were designated as MR-X, where X denotes the retention time in minutes. It should be noted that mass producibility is assured of N-doped rGO because the process involves sonication of a GO solution in a continuous flow manner at 65 °C. A microreactor system is utilized here for demonstration purpose to take advantage of better heat and mass transfer properties of the system, which facilitates tuning of carbon, oxygen and nitrogen contents by controlling retention time.

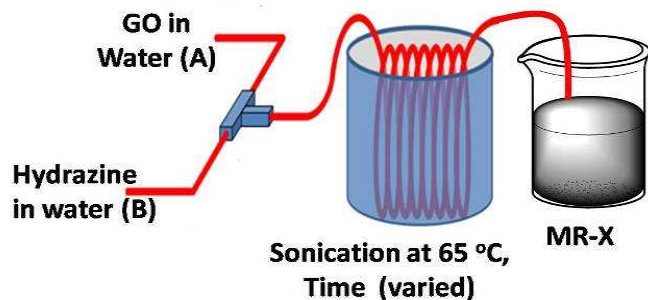


**Fig. 1.** Schematic presentation for synthesis of N-doped rGO (MR-X sample) by continuous microsonochemical process.

This hydrazine reduction of GO resulted in a carbon to oxygen atom ratio of 10.3, which was 2.7 before the reduction, and at the same time led to incorporation of nitrogen, yielding a carbon to nitrogen ratio of 16.1. Intentional nitrogen doping has invariably been accomplished in the process of producing rGO from GO. The methods include thermal annealing with a nitrogen compound,<sup>10</sup> hydrothermal or solvothermal reduction with a nitrogen compound,<sup>11</sup> and simple melamine reduction.<sup>12</sup> The highest nitrogen content achieved by simple hydrazine reduction methods<sup>11d</sup> was 5.2 wt % with a carbon to oxygen atom ratio of 8.4. The effect of retention time on extent of tuned N-doping by MR was investigated by elemental analyses. As shown in Table 1, the nitrogen wt% in rGO exhibited a continuous increase with extended retention time of up to 60 min (MR-60), and eventually reached a plateau of 6.3 %, which is the highest value ever reported in simple solution methods.<sup>11d</sup> Not much difference was observed between the nitrogen contents of traditionally treated rGO-b that was prepared by the usual hydrazine reduction (24 h) method (detailed method in the ESI) and that of MR-30, indicating significant influence of the retention time on N-doping by the microsonochemical reduction. Brunauer–Emmett–Teller (BET) surface area was decreased with increasing N-content in graphene surface may be the cause of agglomeration.

Whilst considering the production of tuned N-doped rGO by microsonochemical method (MR-60), it is of interest to expand the application of N-doped rGO in areas of effective metal-free catalyst for C-H bond activation and comparing the outcomes with reported studies on metal based catalysts and other carbocatalysts.<sup>4a</sup> Oxidation of 1-Methylindoline-2-one, which involved reaction in aqueous phase with *tert*-butyl hydro peroxide (TBHP) as an oxidant<sup>4a</sup> (detailed method in ESI) was selected as a model reaction to evaluate the effect of tuned carbon, oxygen and nitrogen content and also the degree of influence of exfoliation/surface area on the conversion and selectivity. An increase in conversion with higher nitrogen content and with lower oxygen content was observed; however, the surface area (Table 1) had no noticeable effect on the catalytic efficiency. Oxidation of indoline-2-one was also carried out to test the efficiency of N-doped rGO (MR-60) as a catalyst for C-H bond activation. From Table 1, in general, it is obvious that an increased N amount in graphene oxide became less hydrophilic, then the highly N-doped rGO layers tended to agglomerate and decrease the surface area. Therefore, MR-60 revealed the highest nitrogen (6.3%), the lowest oxygen content (4.2%) and the lowest surface area (67  $\text{m}^2\text{g}^{-1}$ ) (Fig. S1 in the ESI), which enabled accomplishment of 96% conversion with 92% selectivity, and formation of 1-methyl indole-2, 3-dione as a major product in 12 h (Table S2). It indicated that the catalytic C-H bond oxidation reactions were dominated by nitrogen content of N-doped rGO, rather than the surface area (Table S2).

**Table 1.** Comparative elemental analysis and XRD of graphite, graphite oxide and reduced graphene oxides powders.

Materials	C	O	H	N	C/O	C/N	C/(O+N)	2 $\theta$	$d_{(100)}$ (Å)	BET surface area [ $\text{m}^2\text{g}^{-1}$ ]
Graphite	99.25	0.009	-	-	-	-	-	26.54	3.36	7.8
GO	41.48	52.32	2.41	-	0.79	-	0.79	9.82	9.0	680
rGO-b	78.72	13.95	1.21	3.41	5.64	23.08	4.55	23.60	3.81	85.7
MR-30	78.54	13.86	0.95	3.54	5.66	22.18	4.51	-	-	130.6
MR-40	82.51	10.31	0.99	4.56	8.02	18.09	5.54	-	-	90.5
MR-50	84.96	7.01	1.02	5.02	12.1	16.92	7.06	-	-	78.3
MR-60	87.01	4.20	1.09	6.34	20.7	13.72	8.25	24.70	3.62	67.1
MR-70	87.02	4.21	1.09	6.35	20.7	13.70	8.25	-	-	66.5

As shown in Fig. S2a (in the ESI), the intensity of N1s peak of MR-60 is higher than that of rGO-b, which is produced by the conventional hydrazine batch process, indicating higher N content in MR-60 platelets. The resolution of deconvoluted N1s peak was achieved into three components centred at 398.1-399.3 eV for pyridinic N, at 399.8-401.2 eV for pyrrolic N, and at 401.1-402.7 eV for graphitic or quaternary N (Fig. S3a in the ESI).<sup>13</sup> Fig. S3a also reveals the nature of nitrogen in rGO-b as mostly pyridinic (~50%) or pyrrolic (~49%) and only a negligible amount of nitrogen (~1%) as graphitic or quaternary (Fig. S3b in the ESI), whereas nitrogen in MR-60 as more substantially graphitic (~20%) (pyridinic:~51% and pyrrolic:~29%). At the same time it is apparent that most of the nitrogen (~99%) was introduced into the graphene edges and only 1% into the basal plane when GO was reduced by the conventional hydrazine method, whereas a substantial amount of nitrogen (~20%) was incorporated into graphene basal plane when GO was reduced by the microsonochemical reduction (MR-60). In the traditional hydrazine treatment, it is known that adjacent layers of GO platelets snap together due to  $\pi$ - $\pi$  interaction<sup>5</sup> as the basal planes near the edges become reduced. As a result, there is narrowing of interlayer distance, which prevents further penetration of hydrazine into the interior, leading to a limited extent of nitrogen doping. However, it is well known that the ultrasound functions by sonochemical process that involves sequential formation, growth and collapse of millions of microscopic vapour bubbles (voids) in the liquid. These rapid and violent implosions generate short-lived regions with highly intensified energetic environment (~5000 °C and ~1000 atm, ~10<sup>9</sup> °C/sec as heating and cooling rates).<sup>14</sup> Such localized hot spots must be visualized as a microreactor in which the energy of sound is transformed into a useful chemical form.<sup>15</sup> In the microsonochemical process, continuous sonication creates hot spots due to bursting microscopic bubbles, which along with the high surface area to volume ratio of microreactor could possibly lead to activation of hydrazine, aiding in dispersion of GO platelets, and enhancement of mass and heat transfer. Consequently, it is hypothesized that combination of these factors must have facilitated diffusion of hydrazine into the interior of GO platelets.

The elemental composition tuning capability of the microsonochemical method is also apparent with respect to carbon to oxygen (C/O) weight ratio as given in Table 1. In the case of the traditional hydrazine treatment (rGO-b), the C/O ratio reached 5.64, when GO with a C/O ratio of 0.79 was treated with hydrazine for 24 h. Whereas, in case of continuous microsonochemical process, the C/O ratio was attained as 5.66, when GO with C/O ratio of 0.79 was treated with hydrazine only for 30 min. Subsequently, the C/O ratio reached 20.7 after 60 min, which far exceeds the highest ever reported C/O ratio of 15.3, that was obtained by treating GO with a mixture of HI and acetic acid for 40 h.<sup>16</sup> XRD (Table 1, Fig. S2b, in the ESI) reveals the interlayer distance for MR-60 as 3.62 Å ( $2\theta = 24.7^\circ$ ), which proves better recovery of the layered structure as further indicated by lowering d-spacing than 3.81 Å of rGO-b. C1s and O1s, XPS spectra further confirm that the delocalized  $\pi$ -conjugation was restored in MR-60 sample (Fig. S2c&d, Fig. S3c-h in the ESI).

HR-TEM image of MR-60 sample (Fig. 2 d-f) shows well oriented graphitic layers (up to 22 layers) that was ~7.8 nm thick (Fig. 2 g), which corresponds to 3.63 Å interlayer distance, consistent with 3.62 Å obtained by XRD measurements. This low interlayer distance of MR-60 was comparable to a d-spacing of 3.64 Å for the reduced GO with no N-doping, obtained by a mixture of HI and acetic acid.<sup>16</sup> From these MR-60 platelets, the selected area electron diffractions pattern (SAED) was performed on this region along [001] zone axis. The diffraction pattern

of MR-60 in Fig. 2h, showed crystalline structure. The first ring came from the (1100) plane and the bright spots corresponding to the (1100) reflections retained the hexagonal symmetry of the [0001] diffraction patterns. The MR-60 platelets with more than six bright hexagonal spots might contain clustered defect arising from oxidation.<sup>16</sup>

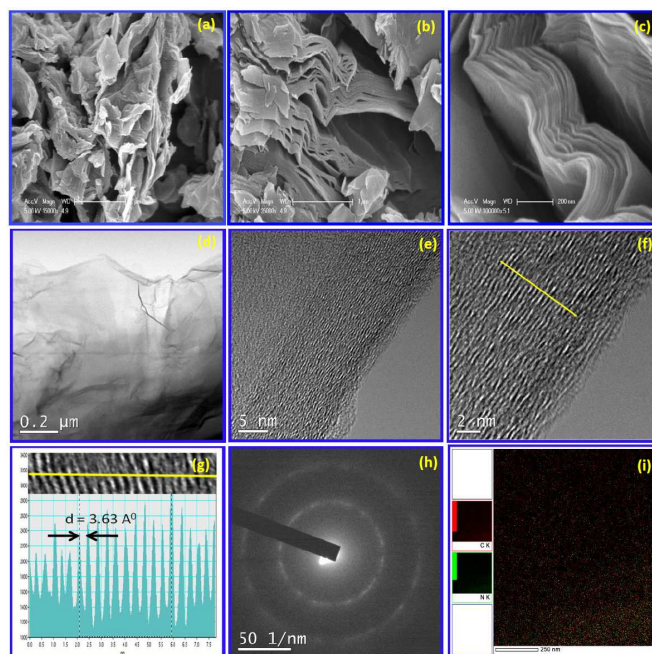


**Fig. 2.** Microscopic analysis of GO, rGO-b and MR-60; (a, b&c) SEM images of GO, rGO-b and MR-60 (d, e&f) TEM image of MR-60 in surface view; cross-section of a stacked graphitic layers of MR-60; (g) d-spacing from stacked MR-60 layers; (h) selected area electron diffraction pattern of MR-60; (i) mixed C and N elemental mapping in nanometer range.

The platelets in MR-60 samples were well dispersed in DMF solvent and remained stable even after 1 month (Fig. S4, in the ESI), which is an additional evidence for the presence of highly deoxygenated graphene platelets. TGA (Fig. S5 a&b, in the ESI) shows that the weight loss by MR-60 is much less (13.2 wt%) when compared to both rGO-b (22 wt%) and GO (80 wt%) when heated to 800°C in nitrogen atmosphere; the analysis reveals high thermal stability of MR-60 presumably due to the higher level of deoxygenation. The scanning electron microscopy (SEM) images of GO, rGO-b and MR-60, were as shown in Fig. S6 a-c, respectively. The layers of rGO-b was relatively ill arranged with the outer layers slightly delaminated, presumably due to stirring, whereas those of MR-60 was well aligned. As these clusters were not fully restored into the hexagonal graphene framework, the MR-60 platelets have inclusions containing a periodic decoration of functional groups. Furthermore, the graphitic laminar structure of stacks of MR-60 platelets could be resolved in the ordered region. The nitrogen and carbon in MR-60 graphene was found to be uniformly distributed not only at the edge but also in the plane of graphene, as evidenced by the TEM elemental mapping in Fig. 2i. At here, it should be pointed out that the microsonochemical method presented here is quite simple to carry out at low temperature (65 °C) and the doping level can simply be controlled by extending retention time.

Electrical conductivity of MR-60 (~9035 S/m) was enhanced by ~5 fold when compared to rGO-b (~1630 S/m) samples (details in ESI). Eventually, the afore-mentioned analytical results demonstrate excellent

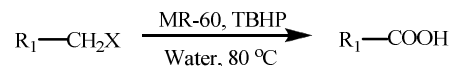
tuning capability of microsonochemical process. To the best of our knowledge, until date, the tuned GO based material has not been reported as an efficient oxidation catalyst under mild condition except for the available report on layered N-doped graphite for oxidation of benzyl alcohol.<sup>4</sup>

Entry	Reactant	Product	% Conversion (% Selectivity)
1			96 (92)
2			73 (74)
3			99 (92)
4			99 (95)
5			99 (97)
6			93 (92)
7			70 (48)
8			99 (99)

**Scheme 1:** Carbocatalytic selective oxidation for syntheses of aromatic and aliphatic ketone products. General conditions: substrate (1.0 mmol), MR-60 catalyst (0.03 g), TBHP (3.0 mmol, 65 % in water), water (3 mL), time 12 h at 80 °C, conversion and selectivity based on GC analysis by using anisole as an internal standard.

After having demonstrated the excellent activity of MR-60 catalyst in the model reaction, we investigated selective oxidation of a series of structurally diverse benzyl and alkyl substituted compounds (Scheme 1). As shown in Scheme 1, excellent yields of corresponding aromatic ketones were typically obtained and compared with the previous reports on metal based catalysts (Table S3, in the ESI). Apart from simple aromatic C-H bond oxidation (Scheme 1, Entry 1-6); the most difficult aliphatic C-H bonds were also selectively oxidized to aliphatic ketone (Scheme 1, Entry 7). The results of selective oxidation demonstrate that MR-60 delivers a much better performance than the best known manganese-containing molecular sieve catalyst (Mn-ALPO-18).<sup>17</sup> Alcohol functionalized C-H bond was selectively converted to ketones (Scheme 1, Entry 8) and results were comparatively good with other types of previously reported carbocatalysts and Pd based metal catalyst (Table S3, Entry 1-8, in the ESI).<sup>18</sup> Aromatic C-H bond oxidation showed better selectivity as compared to non-aromatic C-H bond

oxidation presumably due to  $\pi$ - $\pi$  interactions between aromatic reactant and graphene layer.<sup>4a</sup>



Entry	Reactant	Product	% Conversion (% Selectivity)
1			99 (99)
2			99 (97)
3			99 (98)
4			96 (98)
5			97 (98)
6			99 (98)
7			99 (99)

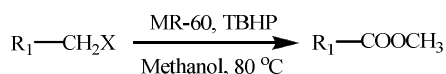
**Scheme 2:** Carbocatalytic selective oxidation for syntheses of aromatic acid products. General conditions: substrate (0.5 mmol), MR-60 catalyst (0.03 g), TBHP (5.0 mmol, 65 % in water), water (1 mL), time 12 h at 80 °C, conversion and selectivity based on GC analysis by using anisole as an internal standard.

A distinct advantage of the MR-60 catalyst against the supported metal catalysts is durable catalytic activity because there is no component to be leached out in the course of a reaction. To test this hypothesis, MR-60 catalyst was recycled six times for ethyl benzene oxidation. There was nearly no change in selectivity only with little decreased conversion, presumably due to incomplete sample recovery in filtration and washing step (Fig. S6 & Table S4 in the ESI). No alteration in N-doping was observed after recycling for six times as confirmed by elemental analysis.

To insure the reaction mechanism for selective C-H bond oxidation, ethyl benzene was chosen as a reactant without oxidant (TBHP), and no reaction was observed, indicating that the catalyst and water oxygen didn't participate in the reaction. On the other hand, when a free-radical scavenger (TEMPO, 10 mmol %) was used along with the reactants including TBHP, the reaction did not occur, which is a direct evidence for the progress of a reaction through free radical mechanism. Moreover, TBHP needs to be activated directly on the surface catalyst for the oxidation reactions, with formation of radicals in the solution (Fig. S7, in the ESI). Similar results were obtained when TBHP was used to oxidize the same substrate in the presence of N-doped graphite, where the reaction is known to proceed via radical mechanism.<sup>4a</sup> After having demonstrated the reaction mechanism that the free-radical intermediate generated peroxide radical, we further investigated selective oxidation of benzyl alcohol and a series of structurally diverse benzyl bromides for synthesis of aromatic acids to understand the substitutional effect. As can be seen in scheme 2, various acids are obtained with excellent yields and selectivity. Apart from simple benzyl alcohol (Scheme 2, Entry 1), *p*-methyl, *p*-fluoro, *p*-chloro, *p*-bromo benzyl bromide, and styrene were selectively converted into the corresponding aromatic acid products

## Green Chemistry

(Scheme 2, Entry 2-7) and these results were comparable with previous reports on metal catalysts (Table S3, Entry 9, in the ESI).<sup>19</sup>



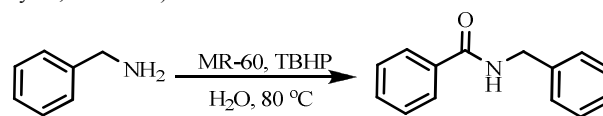
Entry	Reactant	Product	% Conversion (% Selectivity)
1			99 (85)
2			99 (97)
3			99 (99)
4			96 (97)
5			97 (95)
6			99 (95)
7 <sup>a</sup>			99 (99)
8 <sup>a</sup>			99 (99)

**Scheme 3:** Carbocatalytic selective oxidation for syntheses of aromatic ester or ether products. General conditions: substrate (0.5 mmol), MR-60 catalyst (0.03 g), TBHP (5.0 mmol, 65 % in water), MeOH (0.5 mL), time 12 h at 80 °C, (a) without TBHP (R = Phenyl, *p*-methylphenyl, *p*-fluorophenyl, *p*-chlorophenyl, *p*-bromophenyl), conversion and selectivity based on GC analysis by using anisole as an internal standard.

After the successful synthesis of acid, we also checked the solvent effect on the oxidation reaction, where we just replaced water solvent with methanol to ensure better dispersion of biphasic reaction. Nevertheless, completely surprising results were obtained due to conversion of aromatic acid into unexpected aromatic ester. Subsequently, we evaluated other substituted benzyl halides under optimized conditions, and the corresponding esters were similarly produced with nearly complete conversion and excellent selectivity (Scheme 3, Entry 1-6). Synthesis of ester from alcohol has been mostly catalyzed by the metal catalyst (Pd, Au, Ru, Ir, Co) but till to date, there are no available reports on functioning of N-doped graphene oxide as an efficient oxidation catalyst under mild conditions (Table S3, Entry 10, in the ESI). Furthermore, there are no literature reports on direct synthesis of aromatic ester from benzyl bromide.<sup>20</sup> After the successful cross esterification of methanol and various benzyl bromides and alcohol, we were interested in demonstrating the effect of oxidant (TBHP) on esterification reaction. As shown in Scheme 3 (Entry 7&8), aromatic ether was selectively produced from treatment of benzyl alcohol or bromides with methanol in the absence of TBHP and additive for 12 h at 80 °C under optimized conditions; no byproducts were observed in crude reaction mixture. Furthermore, direct synthesis of aromatic ether from benzyl alcohol or bromides using carbocatalyst has not been reported except for the published reports on metal based catalyst with base and additives (Table S3, Entry 11, 12, in the ESI).<sup>21</sup>

Generally, the amide bond is considered as one of the most important linkages in organic-chemistry and constitutes the key

functional group in peptides, polymers, and many natural products and pharmaceuticals.<sup>22</sup> Our MR-60 carbocatalyst also offered reasonable conversion and selectivity for amide bond formation reactions through dihydrogen extrusion (Scheme 4) and the results were comparable with that of precious Ru assisted homogenous metal catalysis (Table S3, Entry 13, in the ESI).<sup>22</sup>



**Scheme 4:** Carbocatalytic selective amide synthesis. General conditions: substrate (1.0 mmol), MR-60 catalyst (0.03 g), H<sub>2</sub>O (3 mL), time 12 h at 80 °C, conversion (75 %) and selectivity (68 %) based on GC analysis by using anisole as an internal standard.

Biphasic medium system (water and organic) with a solid catalyst usually requires a long reaction time, especially when the reaction is carried out in a batch system such as a flask. In the present work, this time-consuming problem was overcome by performing the reaction in a continuous flow capillary microreactor (details are provided in ESI and Fig. S8); the high surface area to volume ratio afforded by microreactor enhanced mass and heat transfer, thereby accelerating the reaction.<sup>23</sup> It is apparent from entry 3 in Table S3 (oxidation of ethylbenzene) that a remarkable reduction in reaction time (40 min from 12 h) was achieved with the use of capillary microreactor system (MR-60 vs. MR-60 in microreactor).

## Conclusion

We have developed a facile technique for C, N and O tuned rGO catalyst by using simple microsonochemical method and propose that rGO material can catalyze selective oxidation. The microsonochemical approach yielded N-doped rGO catalyst (MR-60) with the highest carbon to oxygen ratio (20.7) and the highest nitrogen content (6.3 wt%) during a short reaction time (60 min) ever reported by solution methods. The MR-60 carbocatalyst showed excellent catalytic activity and reusability in the C-H bond activation for selective oxidation reaction under mild reaction conditions. Furthermore, MR-60 is functional group tolerant, inexpensive (novel metal free catalyst) and environmentally gentle catalyst for industrial prospective known until date. The tuned MR-60 possesses the potential of becoming a mass-producible, substitute material for precious metal catalysts. Moreover, the immense potentials of MR-60 could also be extended to diverse applications as electrochemical catalysts, electrode materials, bio-medical applications, green energy and water purification.

## Acknowledgements

This work was supported by a National Research Foundation of Korea (NRF) grant funded by the Korean government (MEST) (2008-0061983).

## References

- 1 E. Gross, H.-C. Liu, Jack, F. D. Toste, G. A. Somorjai, *Nat Chem* 2012, **4**, 947-952.

- 2 W. Huang, J. H.-C. Liu, P. Alayoglu, Y. Li, C. A. Witham, C.-K. Tsung, F. D. Toste, G. A. Somorjai, *J. Am. Chem. Soc.*, 2010, **132**, 16771-16773.
- 3 D. R. Dreyer, H.-P. Jia, C. W. Bielawski, *Angew. Chem. Int. Ed.*, 2010, **49**, 6813-6816.
- 4 a) Y. Gao, G. Hu, J. Zhong, Z. Shi, Y. Zhu, D. S. Su, J. Wang, X. Bao, D. Ma, *Angew. Chem. Int. Ed.*, 2013, **52**, 2109-2113; b) X.-H. Li, M. Antonietti, *Angew. Chem. Int. Ed.*, 2013, **52**, 4572-4576; c) C. Su, M. Acik, K. Takai, J. Lu, S.-j. Hao, Y. Zheng, P. Wu, Q. Bao, T. Enoki, Y. J. Chabal, K. Ping Loh, *Nat. Commun.*, 2012, **3**, 1298.
- 5 S. Park, J. An, J. R. Potts, A. Velamakanni, S. Murali, R. S. Ruoff, *Carbon* 2011, **49**, 3019-3023.
- 6 S. G. Newman, L. Gu, C. Lesniak, G. Victor, F. Meschke, L. Abahmane, K. F. Jensen, *Green Chem.*, 2014, **16**, 176-180.
- 7 J. Swann, Y. Wang, L. Abecia, A. Costabile, K. Tuohy, G. Gibson, D. Roberts, J. Sidaway, H. Jones, I. D. Wilson, J. Nicholson, E. Holmes, *Mol. Biosyst.*, 2009, **5**, 351-355.
- 8 R. A. Maurya, K.-I. Min, D.-P. Kim, *Green Chem.*, 2014, **16**, 116-120.
- 9 a) S. G. Newman, L. Gu, C. Lesniak, G. Victor, F. Meschke, L. Abahmane, K. F. Jensen, *Green Chem.*, 2014, **16**, 176-180; b) S. G. Newman, K. F. Jensen, *Green Chem.*, 2013, **15**, 1456-1472.
- 10 a) X. Li, H. Wang, J. T. Robinson, H. Sanchez, G. Diankov, H. Dai, *J. Am. Chem. Soc.*, 2009, **131**, 15939-15944; b) Feng Ya-Qiang, Tang Fu-Ling, Lang Jun-Wei, Liu Wen-Wen, Y. Xing-Bin, *J. Inorg. Mater.*, 2013, **28**, 677-682.
- 11 a) X. Wang, X. Li, L. Zhang, Y. Yoon, P. K. Weber, H. Wang, J. Guo, H. Dai, *Science* 2009, **324**, 768-771; b) Y. Chang, G. Han, J. Yuan, D. Fu, F. Liu, S. Li, *J. Power Sources* 2013, **238**, 492-500; c) Q. Liu, J. Jin, J. Zhang, *ACS Appl. Mater. Interf.*, 2013, **5**, 5002-5008; d) D. Long, W. Li, L. Ling, J. Miyawaki, I. Mochida, S.-H. Yoon, *Langmuir* 2010, **26**, 16096-16102.
- 12 S.-M. Li, S.-Y. Yang, Y.-S. Wang, C.-H. Lien, H.-W. Tien, S.-T. Hsiao, W.-H. Liao, H.-P. Tsai, C.-L. Chang, C.-C. M. Ma, C.-C. Hu, *Carbon* 2013, **59**, 418-429.
- 13 P. Sungjin, H. Yichen, H. Jin Ok, L. Eui-Sup, B. C. Leah, C. Weiwei, R. P. Jeffrey, H. Hyung-Wook, C. Shanshan, O. Junghoon, K. Sang Ouk, K. Yong-Hyun, I. Yoshitaka, S. R. Rodney, *Nat. Commun.*, 2012, **3**, 638-638.
- 14 K. Prasad, D. V. Pinjari, A. B. Pandit, S. T. Mhaske, *Ultrason. Sonochem.*, 2010, **17**, 409-415.
- 15 R. M. Srivastava, R. A. W. Neves Filho, C. A. da Silva, A. J. Bortoluzzi, *Ultrason. Sonochem.*, 2009, **16**, 737-742.
- 16 M. In Kyu, L. Junghyun, S. R. Rodney, L. Hyoyoung, *Nat. Commun.*, 2010, **1**, 73-73.
- 17 R. Raja, J. Meurig Thomas, *Chem. Commun.*, 1998, 1841-1842.
- 18 P. Zhang, Y. Gong, H. Li, Z. Chen, Y. Wang, *Nat. Commun.*, 2013, **4**, 1593.
- 19 S. Wang, Q. Zhao, H. Wei, J.-Q. Wang, M. Cho, H. S. Cho, O. Terasaki, Y. Wan, *J. Am. Chem. Soc.*, 2013, **135**, 11849-11860.
- 20 a) R. V. Jagadeesh, H. Junge, M.-M. Pohl, J. Radnik, A. Brückner, M. Beller, *J. Am. Chem. Soc.*, 2013, **135**, 10776-10782; b) X.-F. Bai, F. Ye, L.-S. Zheng, G.-Q. Lai, C.-G. Xia, L.-W. Xu, *Chem. Commun.*, 2012, **48**, 8592-8594.
- 21 a) G. Joshi, S. Adimurthy, *Synth. Commun.*, 2011, **41**, 720-728; b) Y. Liu, R. Hua, H.-B. Sun, X. Qiu, *Organometallics* 2005, **24**, 2819-2821.
- 22 L. U. Nordstrøm, H. Vogt, R. Madsen, *J. Am. Chem. Soc.*, 2008, **130**, 17672-17673.
- 23 K. S. Elvira, X. C. i Solvas, R. C. R. Wootton, A. J. deMello, *Nat. Chem.*, 2013, **5**, 905-915.